Development 128, 4449-4461 (2001)
Printed in Great Britain © The Company of Biologists Limited 2001
DEV3490

BMPR-IA signaling is required for the formation of the apical ectodermal ridge and dorsal-ventral patterning of the limb

Kyung Ahn[1], Yuji Mishina[2,3], Mark C. Hanks[4], Richard R. Behringer[2] and E. Bryan Crenshaw III[1,*]

[1]Department of Neuroscience, University of Pennsylvania Medical School, Philadelphia, PA, USA
[2]Department of Molecular Genetics, University of Texas MD Anderson Cancer Center, Houston, TX, USA
[3]Laboratory of Reproductive and Developmental Toxicology, National Institute of Environmental Health Sciences, Research Triangle Park, NC 27709, USA
[4]Procter & Gamble Pharmaceuticals, Mason, OH, USA
*Author for correspondence (e-mail: crenshab@mail.med.upenn.edu)

Accepted 21 August 2001

SUMMARY

We demonstrate that signaling via the bone morphogenetic protein receptor IA (BMPR-IA) is required to establish two of the three cardinal axes of the limb: the proximal-distal axis and the dorsal-ventral axis. We generated a conditional knockout of the gene encoding BMPR-IA (*Bmpr*) that disrupted BMP signaling in the limb ectoderm. In the most severely affected embryos, this conditional mutation resulted in gross malformations of the limbs with complete agenesis of the hindlimbs. The proximal-distal axis is specified by the apical ectodermal ridge (AER), which forms from limb ectoderm at the distal tip of the embryonic limb bud. Analyses of the expression of molecular markers, such as *Fgf8*, demonstrate that formation of the AER was disrupted in the *Bmpr* mutants. Along the dorsal/ventral axis, loss of engrailed 1 (*En1*) expression in the non-ridge ectoderm of the mutants resulted in a dorsal transformation of the ventral limb structures. The expression pattern of *Bmp4* and *Bmp7* suggest that these growth factors play an instructive role in specifying dorsoventral pattern in the limb. This study demonstrates that BMPR-IA signaling plays a crucial role in AER formation and in the establishment of the dorsal/ventral patterning during limb development.

Key words: Apical ectodermal ridge, Bone morphogenetic protein receptor, Dorsal-ventral patterning, Engrailed 1, Limb development, loxP/cre conditional knockout, Mouse

INTRODUCTION

Classical transplantation experiments, and more recently molecular studies, demonstrate that the vertebrate limb is regulated along three cardinal axes; proximal-distal (PD), dorsal-ventral (DV) and anterior-posterior (AP) (Johnson and Tabin, 1997; Martin, 1998). Each of these cardinal axes is regulated by an organizing center within the developing limb. The PD axis is dependent on signals emanating from the apical ectodermal ridge (AER). The AP axis is regulated by the zone of polarizing activity (ZPA) on the posterior margin of the limb. The DV axis is regulated by non-ridge ectoderm. In each case, recent advances have elucidated the molecular mechanisms that mediate the function of these organizing centers. However, much less is known about the mechanisms that establish the formation of these organizing centers. We will address the molecular mechanisms required to establish the AER and DV patterning.

Limbs grow and develop with proximal structures forming first, and then progressively distal structures forming with time. The AER forms as a specialized epithelial structure at the distal DV border of the developing limb bud (Tickle and Altabef, 1999). Classical transplantation experiments demonstrate a crucial role for the AER in limb outgrowth and this, in turn, leads to the proper formation of structures along the PD axis (Saunders, 1948). Removal of the AER very early in limb development drastically stunts the growth of the limb bud. If the AER is removed at progressively later stages of development, then the more distal structures are formed (Saunders, 1948). Fibroblast growth factors (FGFs) mediate the function of the AER. Several FGFs are expressed normally in the AER, including *Fgf2*, *Fgf4*, *Fgf8*, *Fgf9* and *Fgf17* (Cohn et al., 1995; Niswander and Martin, 1993; Sun et al., 2000). Beads soaked in FGFs can largely replace the function of the AER (Niswander et al., 1993), and induce ectopic limbs in ovo (Cohn et al., 1995). Previous transplantation experiments have demonstrated that limb mesoderm induces the AER (Carrington and Fallon, 1984; Saunders and Reuss, 1974). However, the molecular mechanisms that mediate this induction are not well understood.

Complex interactions between ectoderm and mesoderm regulate DV patterning during limb development (Chen and Johnson, 1999). Before limb bud formation, inductive signals from the mesoderm are required to establish DV pattern in the overlying ectoderm of the limb field (Geduspan and

MacCabe, 1987; Geduspan and MacCabe, 1989; Michaud et al., 1997). Using transplantation analyses in chick/quail chimeras, Le Douarin and colleagues demonstrated that signals that ventralize limb ectoderm emanate from the lateral mesoderm, whereas signals that dorsalize limb ectoderm are derived from more medial somitic mesoderm (Michaud et al., 1997). However, the molecular mechanisms that mediate these mesoderm derived signals are unknown.

Once the presumptive limb ectoderm is induced by the mesoderm, it then plays a primary role in specifying DV pattern as the limb bud forms (Carrington and Fallon, 1984; Michaud et al., 1997; Saunders and Reuss, 1974). The molecular mechanisms that regulate DV patterning by the limb ectoderm have been characterized by molecular genetic analyses, which are summarized in Fig. 8A,B. The homeodomain gene, Engrailed 1 (*En1*), is expressed in the ventral ectoderm of the limb, where it specifies ventral limb identity (Davis et al., 1991; Gardner and Barald, 1992; Loomis et al., 1996). Null mutations in the *En1* gene dorsalize the ventral limb ectoderm and subsequently the distal region of the limb (Cygan et al., 1997; Loomis et al., 1996; Loomis et al., 1998). These genetic analyses suggest a model in which *En1* is the first step in specifying DV patterning in the ectoderm of the limb (Fig. 8B). Knockout analyses demonstrate that *En1* specifies ventral limb identity, at least in part, by suppressing the expression of the growth factor, *Wnt7a* (Cygan et al., 1997; Loomis et al., 1998). *Wnt7a* expression is normally restricted to the dorsal ectoderm (Dealy et al., 1993; Parr et al., 1993), and null mutations in the *Wnt7a* gene give a double ventral phenotype, which includes the formation of ventral foot pads on the dorsal limb instead of claws and ventralization of dorsal muscles and tendons (Parr and McMahon, 1995). Therefore, DV patterning in the limb ectoderm is specified by domains of *En1* expression ventrally, and *Wnt7a* expression dorsally.

Classical transplantation experiments demonstrate that once DV patterning is established in the limb ectoderm, this ectodermal DV pattern is subsequently conferred upon the underlying mesoderm, at least in the distal limb region (Chen and Johnson, 1999). Molecular analyses suggest the model that ectodermal induction of the underlying limb mesoderm is mediated by *Wnt7a*, which has been shown to induce the LIM-domain factor, *Lmx1b*, in the dorsal mesoderm of the limb (Riddle et al., 1995; Vogel et al., 1995). Null mutations in the *Lmx1b* gene lead to loss of dorsal limb phenotype in mouse and humans (Chen et al., 1998; Dreyer et al., 1998). Therefore, the molecular mechanisms regulating DV patterning by the ectoderm during later stages of limb development are well characterized. However, little is known about the initial phase of limb development in which the mesoderm establishes DV patterning in the overlying pre-limb ectoderm.

We now describe our analyses of a conditional knockout of the most widely expressed type I BMP receptor, BMPR-IA. We specifically abrogated expression of BMPR-IA in the pre-hindlimb ectoderm to determine the role of BMP signaling during limb ectoderm development. BMP receptors are serine/threonine kinases that require both a type I and type II receptor subunit to function efficiently (Massague, 1998). Previous knockout analyses have demonstrated that BMPR-IA, encoded by the *Bmpr* gene (*Bmpr1a* – Mouse Genome Informatics), plays a crucial role in BMP signaling. A null mutation of the *Bmpr* gene results in early embryonic lethality around the time of gastrulation (Mishina et al., 1995). Therefore, genetic analyses of BMPR-IA function during limb development requires a conditional knockout of the gene. To overcome the early embryonic lethal phenotype of the *Bmpr* knockout (Mishina et al., 1995), we used the loxP/Cre approach to induce tissue-specific mutations in the *Bmpr* gene (Nagy, 2000).

Using the loxP/Cre mutagenesis approach, we demonstrate that BMP signaling is required for the formation of the organizing centers that regulate PD and DV patterning in the limb. Abrogation of BMPR-IA signaling interferes with the formation of the AER, and abolishes the expression of FGFs that mediate AER function, as well as other AER molecular markers. Surprisingly, the *Bmpr* conditional knockout results in the formation of double dorsal hindlimbs. This alteration dramatically affects the overall expression of DV regulatory genes; *En1* gene expression is lost in ventral limb ectoderm, and ectopic expression of *Wnt7a* and *Lmx1b* is observed. Finally, we examine the expression profile of the BMPR-IA ligands, BMP4 and BMP7, which are detected early in the lateral mesoderm at a time in which the mesoderm induces DV pattern in the overlying ectoderm. These data demonstrate that BMP signaling is required to establish DV patterning in the limb ectoderm. Furthermore, this is the first demonstration that BMP signaling is required for the formation of critical organizing centers during limb development.

MATERIALS AND METHODS

Generation of transgenic and mutant mouse pedigrees

The null mutation of the *Bmpr* gene was published previously (Mishina et al., 1995). Alleles of the *Bmpr* gene (floxP and floxP-neo) containing loxP sites flanking exon 2 (floxed alleles) were generated as described in Mishina et al. (Y. M., M. C. H. and R. R. B., unpublished). Briefly, a PGK-neo cassette flanked by loxP sites was introduced into intron 2 of *Bmpr* and a third loxP site marked with a *Nhe*I site was introduced into intron 1. The initial targeting event created the floxP-neo allele (Fig. 1D). Mice heterozygous for floxP-neo were mated with CMV-Cre mice (Arango et al., 1999) and resulting progeny were screened by Southern blot for those containing the floxP allele (see Fig. 1D and Southern blot analyses described below).

The *Brn4-Cre* was generated using a 5.6 kb *Sal*I-*Bam*HI fragment encompassing the 5′ flanking regions of the *Brn4* gene, whose 3′ end falls 14 bp 3′ of the initiator methionine. This promoter region was fused to the Cre recombinase gene and polyA sequences from pOG231 (a generous gift of S. O'Gorman, Salk Institute). The transgenic construct was introduced into CD-1 mice using standard transgenic techniques (Hogan et al., 1994). Three viable transgenic founders were generated. Two of these demonstrated tissue-specific recombination, including the *Brn4-Cre* pedigree, designated bcre-32, used in all studies described in this paper. The third pedigree, designated bcre-23, appears to be expressed during early embryogenesis, and has been used as a 'deletor' strain in other studies (Cho et al., 2001). We have not detected expression of the endogenous *Brn4* gene (Phippard et al., 1999; Phippard et al., 1998) or transgenes containing the ~6 kb *Brn4* flanking region (Heydemann et al., 2001) in the limb. The

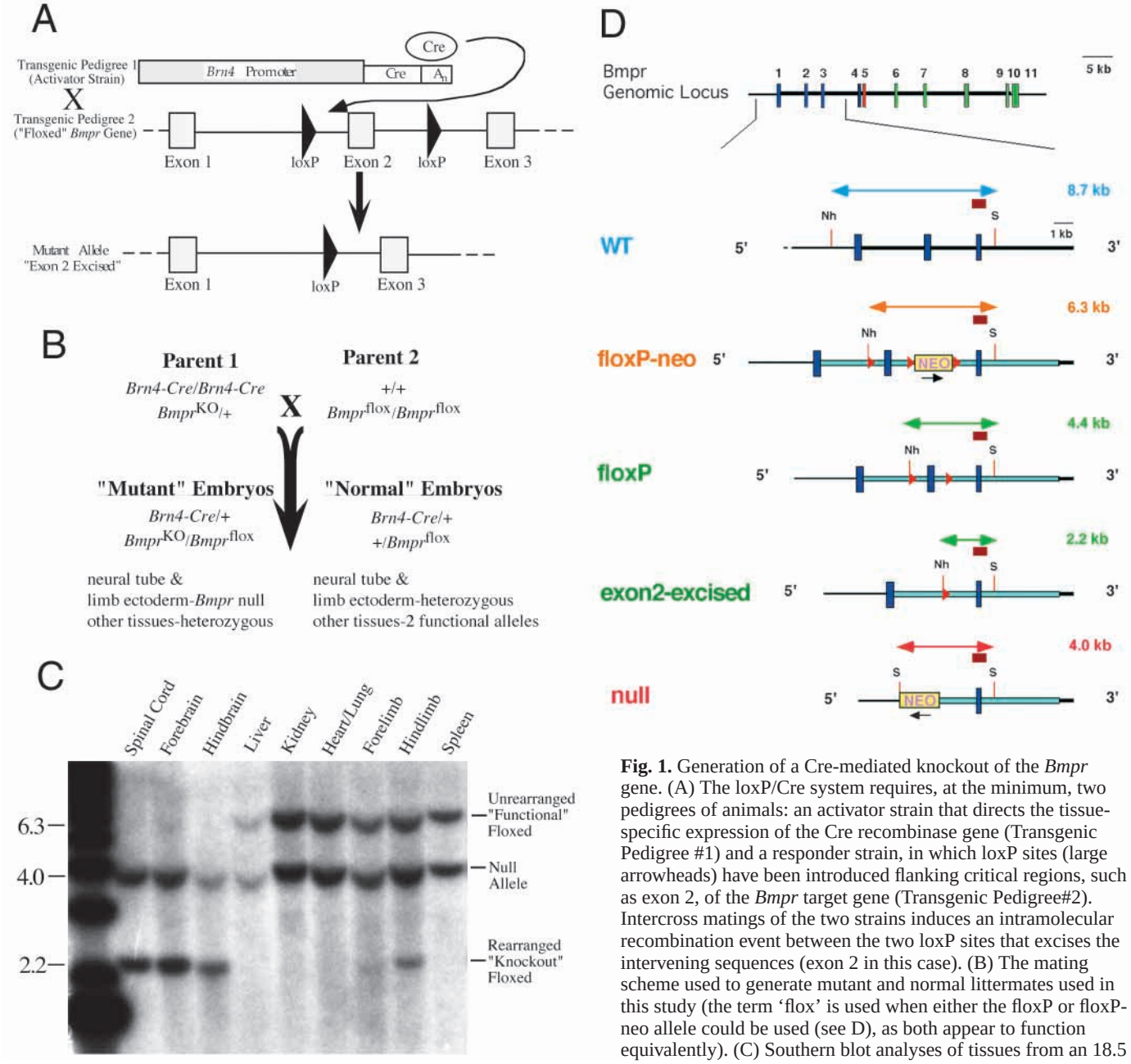

Fig. 1. Generation of a Cre-mediated knockout of the *Bmpr* gene. (A) The loxP/Cre system requires, at the minimum, two pedigrees of animals: an activator strain that directs the tissue-specific expression of the Cre recombinase gene (Transgenic Pedigree #1) and a responder strain, in which loxP sites (large arrowheads) have been introduced flanking critical regions, such as exon 2, of the *Bmpr* target gene (Transgenic Pedigree#2). Intercross matings of the two strains induces an intramolecular recombination event between the two loxP sites that excises the intervening sequences (exon 2 in this case). (B) The mating scheme used to generate mutant and normal littermates used in this study (the term 'flox' is used when either the floxP or floxP-neo allele could be used (see D), as both appear to function equivalently). (C) Southern blot analyses of tissues from an 18.5 dpc embryo demonstrate that the *Brn4-Cre* transgene efficiently mediates the rearrangement of the floxP-neo allele of the *Bmpr* gene (see D for the structure of this allele). In tissues derived from the neural tube, such as spinal cord, hindbrain and forebrain, efficient rearrangement of the floxP-neo allele results in a conversion of the 6.3 kb fragment to a 2.2 kb fragment; the null allele yields a 4.0 kb fragment. The small amount of Cre-mediated rearrangement in the limbs results from the ectodermally derived cells in the limbs that express the *Brn4-Cre* transgene (see Fig. 2); the majority of the limb derives from mesenchymal tissue that does not express the *Brn4-Cre* transgene. Labeled size standard (lane 1) is 1 kb DNA Ladder (Life Technologies); sizes of hybridized bands (kb) are given (left). (D) To introduce loxP sites (arrowheads) into the first and second intron, a targeting vector was engineered to contain one loxP site in the first intron, and a *neo*^{r} gene flanked by loxP sites in the second intron; successful targeting of this construct resulted in the floxP-neo allele depicted in this panel. The residual *neo*^{r} gene in the second intron of the floxP-neo allele apparently did not interfere with the function of the gene, as no discernible phenotype was detected in mice homozygous for this allele. An allele in which the *neo*^{r} gene was specifically removed (floxP) was generated by partial excision of the locus with Cre recombinase (Y. M., M. C. H. and R. B., unpublished). No differences in phenotype were observed whether we used the floxP-neo or the floxP allele. Box (red) above exon 3 of modified alleles corresponds to H23 probe used to genotype *Bmpr* pedigrees. Nh, *Nhe*I; S, *Sac*I.

mating scheme used to generate mutant and normal littermates used in this study is shown in Fig. 1B. Animals that were hemizygous for the *Brn4-Cre* transgene (Fig. 1B; Parent#1) were also used in this study. The ROSA reporter pedigree was a generous gift from P. Soriano (Hutchinson Cancer Center, Seattle, WA).

Southern analysis of Cre-mediated rearrangement of *Bmpr* gene

Genomic DNA was isolated from the tissues indicated in Fig. 1C from an 18.5 dpc embryo, digested with *Nhe*I/*Sac*I, and probed with the H23 probe, which encompasses the third exon (Fig. 1D; box above exon 3 of modified alleles). Each of the *Bmpr* alleles and the Cre-mediated rearrangements of the alleles can be distinguished by Southern analyses of genomic DNA using this strategy.

Histological techniques

Staining for *lacZ* expression was accomplished as described previously (Phippard et al., 1999). Histological analyses of neonatal and adult limbs were accomplished by Hematoxylin and Eosin staining of paraffin sections. When necessary, the limbs were decalcified using Cal ExII (Fisher Scientific). In situ hybridization was accomplished by a modification (T. A. Sanders and C. W. Ragsdale, unpublished) of previously described techniques (Wilkinson, 1992). The mouse *Wnt7a* and *Shh* probes were a kind gift from Andrew McMahon (Parr et al., 1993; Echelard et al., 1993); the mouse *Lmx1b* probe was a kind gift from Randy Johnson (Chen et al., 1998); and the mouse *En1* probe was kind gift from Alexandra L. Joyner (Logan et al., 1992). The *Fgf8*, *Fgf4*, *Bmp2*, *Bmp4* and *Bmp7* probes were generated by PCR amplification of ~0.5 kb regions of the cDNAs that do not cross hybridize.

Phospho-SMAD1 immunohistochemistry

Immunohistochemical analyses were carried out on paraffin sectioned material (7 μm) that had been fixed overnight in 4% paraformaldehyde/phosphate-buffered saline at 4°C prior to embedding in paraffin. Sections were processed by immunoperoxidase labeling using the Vectastain ABC Kit (Vector Labs). The immunoperoxidase signal was amplified with the TSA Indirect Tyramide Signal Amplification Kit (Perkin Elmer Life Science) according to the manufacturer's instructions with the following modifications. For antigen unmasking, sections on slides were heated in a microwave oven in 10 mM sodium citrate pH 6.0 for 4 minutes. Microwave power settings were adjusted to maintain temperature just below boiling during heating. The sections were then treated to quench endogenous peroxidase activity with 2% H_2O_2. The specimens were blocked in 5% normal goat serum for 1 hour at room temperature and incubated overnight at 4°C with the Phospho-Smad1 antibody (Cell Signalling Technology) diluted 1:3000 in 5% normal goat serum. The specimens were then incubated in 0.05% blocking reagent supplied in the tyramide kit for 30 minutes at room temperature to further eliminate nonspecific binding. All further incubations were done in the 0.05% blocking reagent as per manufacturer's instructions.

RESULTS

Generation of a conditional mutation in the *Bmpr* gene

A transgenic mouse pedigree was generated that contained loxP sites in the first and second introns of the *Bmpr* gene (Fig. 1). This modification generated no apparent phenotype in the resulting animals. However, the *Bmpr* gene was now susceptible to conditional inactivation in transgenic animals expressing the Cre recombinase gene. Cre-mediated recombination between the loxP sites removes the second exon of the gene, which encodes roughly a third of the extracellular domain of the receptor within the ligand-binding domain. RNA splicing between the first and third exons results in a frame-shift, therefore further ensuring that Cre-mediated excision will result in a null allele. Mice homozygous for the 'exon2-excised' deletion die without gastrulating, which is identical to the original *Bmpr* null mutant phenotype (Mishina et al., 1995).

Tissue-specific expression of the Cre recombinase gene was driven by the *Brn4/Pou3f4* promoter region in a *Brn4-Cre* transgenic pedigree (Fig. 1A). Previous analyses demonstrated that the *Brn4* proximal 5′ flanking region directs expression to the neural tube (Heydemann et al., 2001). The *Brn4-Cre* pedigree used in this study efficiently induced Cre-mediated rearrangement of the *Bmpr* gene in tissues derived from the neural tube, such as spinal cord, hindbrain and forebrain (Fig. 1C-D). In addition, Southern analyses and the mutant limb phenotype demonstrated that this *Brn4-Cre* pedigree was ectopically expressed in the limbs (Fig. 1C-D). We have not detected expression of the endogenous *Brn4* gene (Phippard et al., 1999; Phippard et al., 1998) or transgenes containing the ~6 kb *Brn4* flanking region (Heydemann et al., 2001) in the limb. Therefore, the ectopic expression of the *Brn4-Cre* transgene in the ventrolateral ectoderm encompassing the limb field is probably a consequence of the site of transgene integration. This transgene integration site does not appear to have interrupted a gene necessary for limb development, because the transgene can be homozygosed without any detectable limb phenotype. Furthermore, molecular markers of limb development are not affected in non-mutant animals containing the *Brn4-Cre* transgene.

Cre-mediated induction of mutation eliminates BMP signaling by 10.0 dpc

To determine the spatial and temporal expression of the *Brn4-Cre* pedigree in the limb, we intercrossed the *Brn4-Cre* pedigree with the ROSA reporter strain, which activates the expression of the *lacZ* gene upon Cre-mediated recombination (Soriano, 1999). As shown in Fig. 2A, *Brn4-Cre*-mediated expression of *lacZ* is initially detected at 9.75 dpc in the ventrolateral ectoderm in a region encompassing both of the embryonic limb anlage. At this stage of embryogenesis, the forelimb bud has begun to form, but the hindlimb bud, which typically forms about a half a day later than the forelimb, has not formed yet (Fig. 2A). The expression of the *Brn4-Cre* transgene is restricted to the ectoderm of the limb with the highest degree of *lacZ* reporter expression detected in the AER. Abundant *lacZ* reporter expression was also detected in the ventral limb ectoderm, and some expression was detected in the dorsal limb ectoderm (Fig. 2B). Significant *Brn4-Cre*-mediated induction of reporter transgene expression was detected at the earliest stages of hindlimb bud formation (Fig. 2C). The induction of reporter gene expression increased in the limb ectoderm, particularly in the pre-AER region, as the limb develops (Fig. 2C-E). The overall pattern of Cre-mediated *lacZ* expression was identical in the forelimb at this stage, but the abundance of reporter expression was reduced in comparison to the hindlimb (Fig. 2G,H). These data demonstrate that the *Brn4-Cre* transgene expression is activated simultaneously throughout the ventrolateral ectoderm encompassing the limb fields/bud. However, the forelimb bud begins to form before Cre-mediated expression, whereas the hindlimb forms after Cre-mediated *lacZ* expression is induced.

To assess directly the loss of BMP signaling, we examined the degree of phosphorylation of SMAD1 (phospho-SMAD1), which is phosphorylated by BMPR-IA signaling. At 9.75 dpc, phospho-SMAD1 immunopositive cells can be detected in

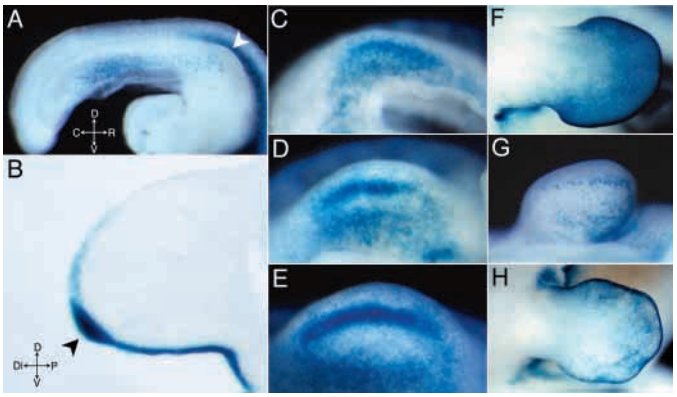

Fig. 2. ROSA reporter analyses demonstrated that Cre-mediated recombination occurred in the limb ectoderm prior to hindlimb bud formation, but after the forelimb bud had begun to form. Cre-mediated rearrangement of the ROSA reporter results in activation of *lacZ* expression and elucidates the temporal and spatial domain of ectopic *Brn4-Cre* gene expression in the embryonic limb. (A) This panel depicts a 9.75 dpc embryo that is doubly transgenic for the ROSA reporter and the *Brn4-Cre* transgene. The initial expression of the ROSA reporter was detected in ventrolateral ectoderm at a time in which the forelimb bud had begun to form (white arrowhead), but before initial hindlimb bud formation, which occurred several hours later. Arrows designate major axes: D, dorsal; V, ventral; R, rostral; C, caudal. (B) Vibratome section (100 μm) of a 10.5 dpc hindlimb demonstrated that Cre-mediated *lacZ* expression was restricted to the ectoderm of the limb. Cre-mediated *lacZ* expression was highest in the AER, although significant levels of expression were found in the ventral ectoderm. Limited induction of expression occurred in the dorsal limb ectoderm. Arrows designate major axes: D, dorsal; V, ventral; Di, distal; P, proximal (C-E). These panels demonstrate Cre-mediated expression of *lacZ* from the earliest stages of hindlimb formation in embryos sacrificed at 10.0 dpc. As the hindlimb bud grows, expression becomes particularly high in the pre-AER region at the distal tip of the limb. The hindlimbs depicted represent the typical variability in age of embryos sacrificed at 10.0 dpc; hindlimbs were ordered progressively based upon limb bud size. (F) By 12.0 dpc, the hindlimb expresses the activated *lacZ* throughout much of the dorsal ectoderm, as well as the ventral ectoderm and AER. (G) Both the extent and timing of ROSA reporter activation are different in the forelimb. At 10.25 dpc, the forelimb attains a more advanced limb bud stage than the hindlimb, but the degree of ROSA reporter activation is reduced when compared with earlier limb bud stages of the hindlimb (compare with E). (H) At 12.0 dpc, the degree of ROSA reporter is reduced compared to the hindlimb (compare with F). However, there is considerable induction of the ROSA reporter gene in the AER at this stage of embryogenesis.

normal embryos throughout the ventral mesoderm of the embryo, and is particularly high in the most ventral regions of the embryo and in the ventral wall of the coelom (Fig. 3A). Higher magnification view (Fig. 3B) demonstrates the phospho-SMAD1 signal is detected at high levels in both the ectoderm and the mesoderm. The specificity of the immunostaining is demonstrated by the detection of phospho-SMAD1 immunopositive cells in regions that have previously shown to express high levels of BMP growth factors, such as the dorsal neural tube (Fig. 3C), ventral mesoderm (Fig. 3A), the neural retina (Fig. 3M) and the dorsal hindbrain (Fig. 3N). Furthermore, absence of the primary antibody results in complete loss of immunolabeling (data not shown). In 9.75 dpc *Bmpr* mutants, the pattern of phospho-SMAD1 immunostaining looks similar to that found in normal embryos (Fig. 3D,E). Most ectodermal cells demonstrate robust immunolabeling. However, unlike in normal embryos, a rare ectodermal cell can be identified that has little or no immunostaining (Fig. 3E). Although the *Brn4-Cre* transgenic pedigree eliminates BMPR-IA in the neural tube, phospho-SMAD1 staining is still detected in the dorsal neural tube. This result is consistent with the observation that we do not detect phenotypic changes in the dorsal neural tube of these mice (data not shown), and suggest that functional redundancy of BMP receptor function occurs in the neural tube, but not the limb ectoderm.

In the normal embryos at 10.0 dpc, nuclear phospho-SMADl immunolabeling is detected at high levels in both the mesoderm and the ventral ectoderm of the limb (Fig. 3G,H), but not in the dorsal limb ectoderm (Fig. 3G, inset). However, in the 10.0 dpc mutant animals, phospho-SMAD1 labeling is not detectable in the vast majority of ectodermal cells, although robust staining is still detected in adjacent mesodermal cells (Fig. 3J,K). The loss of phospho-SMAD1 immunolabeling is specific for limb ectoderm, because we do not detect changes in the dorsal neural tube (Fig. 3L), the lateral mesoderm (Fig. 3J), dorsal hindbrain or neural retina (data not shown).

To corroborate that BMP signaling is abrogated at 10.0 dpc, we examined the expression of *Msx2*, whose expression is often induced by BMP signaling (Hogan, 1996). *Msx2* expression is not detected in mutant limb ectoderm at 10.0 dpc, although its expression is still detected in the dorsal neural tube (Fig. 3O,P). No differences in *Msx2* expression were detected at 9.75 dpc (data not shown). Attempts to detect loss of BMPR-IA expression directly by in situ hybridization or by immunohistochemistry did not yield reliable results. However, three different criteria, namely, ROSA reporter expression, phosphorylation of SMAD1 and expression of *Msx2*, demonstrate that the *Bmpr* gene is mutated resulting in loss of BMP signaling between 9.75 dpc and 10.0 dpc.

Limb phenotype in *Bmpr* mutants

Conditional inactivation of the *Bmpr* gene using the *Brn4-Cre* transgenic pedigree resulted in a severe limb phenotype (Fig. 4). Although the phenotype was variable, the most severely affected animals (8/42 hindlimbs) demonstrated complete agenesis of the hindlimb (Fig. 4A). The forelimbs typically demonstrated subtle malformations, which occasionally resulted in an ectopic distal phalange (Fig. 4B,D). However, the hindlimbs of the mutant animals were more severely affected, presumably because the *Brn4-Cre* transgene was expressed before limb bud formation in the hindlimb, but after initial forelimb bud formation. The mutant hindlimbs were grossly malformed (Fig. 4C,F,G,I). A common feature of the hindlimb malformations was polysyndactyly (Fig. 4C,F,G,I). This phenotype included fusion of digits (syndactyly), as well as partial duplication of distal segments of the digits (Fig. 4F,G,I). The typical hindlimb had fewer digits (Fig. 4C,F). However, the mutant limbs rarely demonstrated supernumerary (polydactyly) digits (Fig. 4G,I). In addition, hematoma at the distal tips of the digits was commonly observed (Fig. 4C). Transverse sections through the hindlimbs of moderately affected mutants demonstrated a loss of ventral structures (Fig.

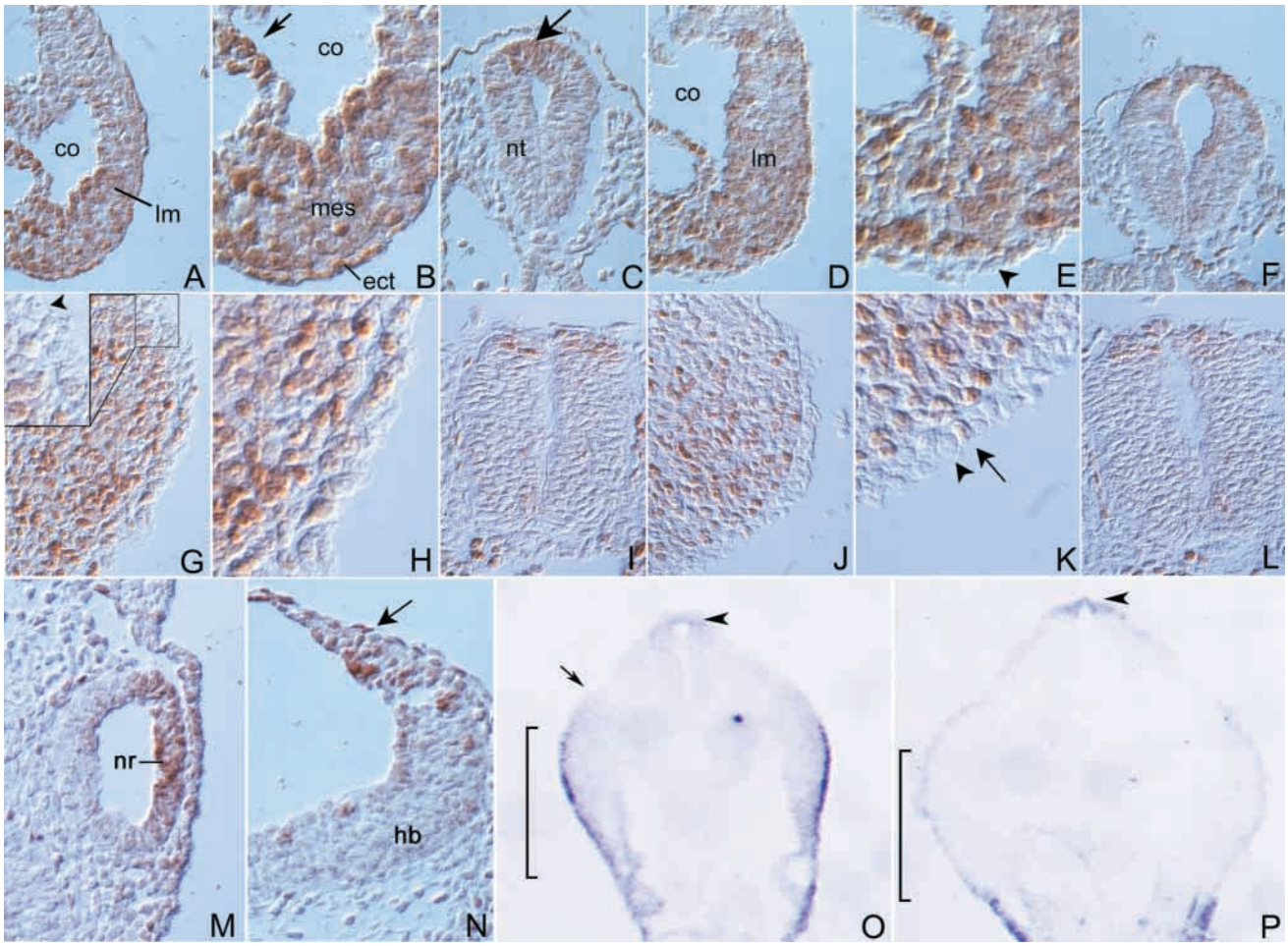

Fig. 3. Phospho-SMAD1 immunolabeling and *Msx2* gene expression demonstrate loss of BMPR-IA signaling between 9.75 and 10.0 dpc in limb ectoderm. (A) Transverse section of a 9.75 dpc normal embryo demonstrating phospho-SMAD1 immunolabeling in the lateral mesoderm (lm) and the overlying ectoderm in the hindlimb field. Strong immunolabeling is detected on the ventral side of the coelom (co), and an overall gradient of labeling is detected with the highest labeling in the most ventral region of the embryo. (B) A higher magnification view of A. (C) Phospho-SMAD1 labeling is detected preferentially in the dorsal neural tube of normal embryos adjacent to the roofplate, which is a rich source of BMP factors. (D) Mutant embryo section corresponding to the normal embryos shown in A. (E) A higher magnification view of D. At this stage, only an occasional ectodermal cell shows reduced levels of phospho-SMAD1 immunolabeling, as indicated by the arrowhead. (F) Phospho-SMAD1 labeling is detected preferentially in the dorsal neural tube of mutant embryos, suggesting functional redundancy of BMP receptor function in the neural tube of these embryos. (G) Transverse section through hindlimb bud of a 10.0 dpc normal embryo demonstrating phospho-SMAD1 immunolabeling in the lateral mesoderm and the overlying ectoderm. Inset demonstrates that phospho-SMAD1 immunolabeling is low or undetectable in the dorsal ectoderm (see arrowhead). (H) Higher magnification view of G, showing the predominantly nuclear immunolabeling. (I) Phospho-SMAD1 immunolabeling in dorsal neural tube of 10.0 dpc normal embryo. (J) Phospho-SMAD1 labeling in a section of mutant embryo demonstrates that immunolabeling is not detected in most ectoderm cells, but robust immunolabeling is detected in the underlying mesoderm. Section comparable with that shown in G. (K) Higher magnification view of J demonstrates that only an occasional cell demonstrates phospho-SMAD1 immunolabeling in the mutant ectoderm (arrow), whereas the vast majority of ectodermal cells are not immunolabeled at 10.0 dpc (arrowhead). (L)Phospho-SMAD1 immunolabeling in the dorsal neural tube of mutant 10.0 dpc embryo. (M) Phospho-SMAD1 immunolabeling is detected in neural retina of 9.75 dpc eye. (N) Phospho-SMAD1 immunolabeling in dorsal hindbrain of 9.75 dpc embryo. (O) In situ hybridization demonstrates that expression of *Msx2* at 10.0 dpc is detected in ventral hindlimb (bracket, transverse plane of section). Arrow indicates the border between lateral and paraxial mesoderm; arrowhead indicates *Msx2* expression in the dorsal midline. (P) Expression of *Msx2* in the mutant is abolished in the ventral hindlimb indicating that BMP signaling has been abrogated (bracket corresponds to region that normally expresses *Msx2*; arrowhead indicates *Msx2* expression in the dorsal midline).

4H,I,L,M). This was most clearly illustrated by the loss/transformation of the prominent ventral flexor digitorum profundus tendon, and an overall mirror image symmetry of the mesenchyme in the dorsal/ventral plane (Fig. 4H,I,L,M). Skeletal preparations demonstrated a loss of the sesamoid process, which is a ventral bone structure (Fig. 4J,K). Additionally, malformed hair follicles were found on both the ventral and dorsal surfaces of the foot, whereas follicles were normally restricted to the dorsal limb (data not shown). Finally, eccrine glands, which were normally found on the ventral side of the limb, were drastically reduced in number on the ventral side of the mutant hindlimb (data not shown). These data

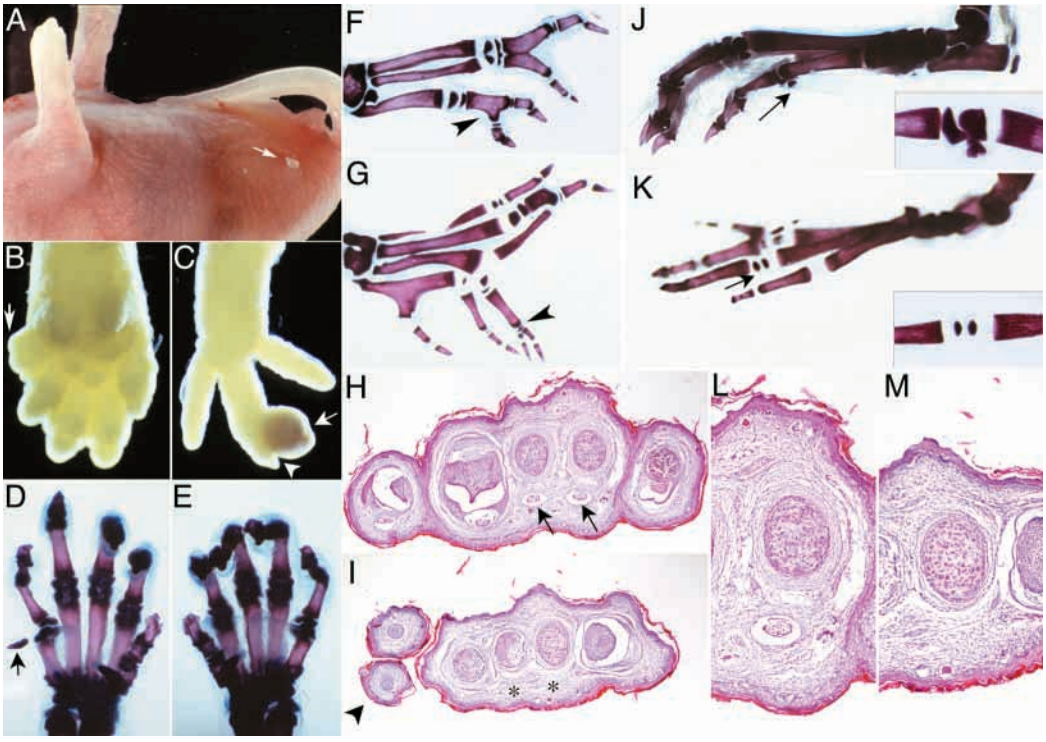

Fig. 4. Cre-mediated inactivation of the *Bmpr* gene in the limb resulted in severe abnormalities in the hindlimb and more subtle defects in the forelimb. Although variability existed in the hindlimb phenotype, it was typically quite severe. (A) The most severe phenotype resulted in complete agenesis of the hindlimb in approximately one-fifth of the mutants (8/42 hindlimbs), as depicted in this P0 neonate (arrow). (B) Forelimb development was comparatively normal, although malformations, including partial polydactyly (arrow) and dysplastic digits (data not shown), were detected. (C) A representative malformation of the hindlimb, including a partial duplication of the distal region of the digit (arrowhead) and hematoma at the tip of the digits (arrow). The proximal skeletal elements of the digit (metatarsals and proximal phalanges) were typically reduced in number with the majority of the hindlimbs containing two (11/42) or three (13/42) digits. (D) A cleared whole-mount preparation of the forelimb of a *Bmpr* mutant was stained with Alizarin Red and Alcian Blue to visualize the bone structure. This panel demonstrates a partial polydactylous digit composed of a distal phalange, including the nail. (E) Forelimb from opposite side of animal depicted in D. (F) A mutant skeletal preparation demonstrates a reduction in digit number associated with syndactyly and a partial duplication (arrowhead) of the digits more distally. (G) Skeletal preparation of a rare polydactylous hindlimb demonstrating four proximal metatarsals, but seven distal phalanges. (H) A transverse section through a normal hindlimb at the level of the digits reveals the typical dorsal/ventral organization of the musculature and tendons. Arrows indicate the flexor digitorum profundus tendon in two of the digits. (I) A similar section through a mutant hindlimb demonstrated a double dorsal phenotype. The flexor digitorum profundus tendon did not display the prominent phenotype observed in the normal animal (asterisks), and the musculature formed an overall mirror-image symmetry unlike the obviously polarized structure of the normal animal. The hindlimb depicted in this panel is comparatively normal when compared to the distribution of mutant hindlimb phenotypes observed in the mutants. However, this mutant hindlimb still demonstrated a partial duplication of the digit, which is displaced ventrally (arrowhead) compared with the other digits. (J) Lateral view of normal hindlimb skeletal prep from a normal P10 mouse, Arrow indicates the sesamoid process, which is a ventral structure. The inset is a higher magnification view of the sesamoid process. (K) Lateral view of mutant P10 hindlimb demonstrating lack of sesamoid process. (L) A higher magnification view of normal digit transverse section indicated by right arrow in H. (M) A higher magnification view of the mutant digit for comparison to L (area indicated by right asterisk in I).

demonstrate that the morphology of the hindlimb displayed a double dorsal phenotype.

Formation of apical ectodermal ridge is disrupted in *Bmpr* mutants

To determine the molecular genetic basis for the observed phenotype, we queried each of the cardinal limb axes using molecular markers. *Fgf8* is expressed in the AER and pre-AER, where it mediates, in part, the organizing function of the AER along the proximal/distal axis (Crossley et al., 1996; Mahmood et al., 1995; Sun et al., 2000; Vogel et al., 1996). *Fgf8* expression was initially detected in the hindlimb field of normal littermates at approximately 10.0 dpc (Fig. 5A). We detected little, if any, *Fgf8* expression in the hindlimb of mutant embryos at this stage of embryogenesis (Fig. 5B). Later in embryogenesis (10.5-11.5 dpc), we detected *Fgf8* expression in mutant hindlimbs, but the expression varied considerably from virtually complete loss of expression (Fig. 5D) to largely intact expression along the distal rim of the limb with short breaks (Fig. 5F). In Fig. 5E, we depict a mid-range phenotype with large stretches of *Fgf8* expression along the distal rim interspersed with regions that do not express *Fgf8*.

The variability of *Fgf8* expression in the mutant hindlimb buds reflected the variability that we observed in the hindlimb phenotype from complete agenesis of the hindlimb to a largely intact hindlimb. Table 1 indicates the extent of variability in the domain of *Fgf8* expression in embryos of ages 10.25-11.5 dpc. Embryos were scored by quartiles between ‘0’ and ‘4’, according to the length of *Fgf8* expression along the distal rim of the hindlimb. None of the mutant embryos scored in Category ‘4’ which corresponded to normal *Fgf8* pattern (as depicted in Fig. 5C). The majority of embryos scored in Categories ‘1’ and ‘2’, corresponding to approximately a quarter to a half of the length of Fgf8 expression detected in normal embryos. Overall, a total of 8/35 embryos scored in Category ‘0’, corresponding to no expression or only a focal patch of expression (Fig. 5D). The number of embryos in Category ‘0’ corresponded approximately with the number of

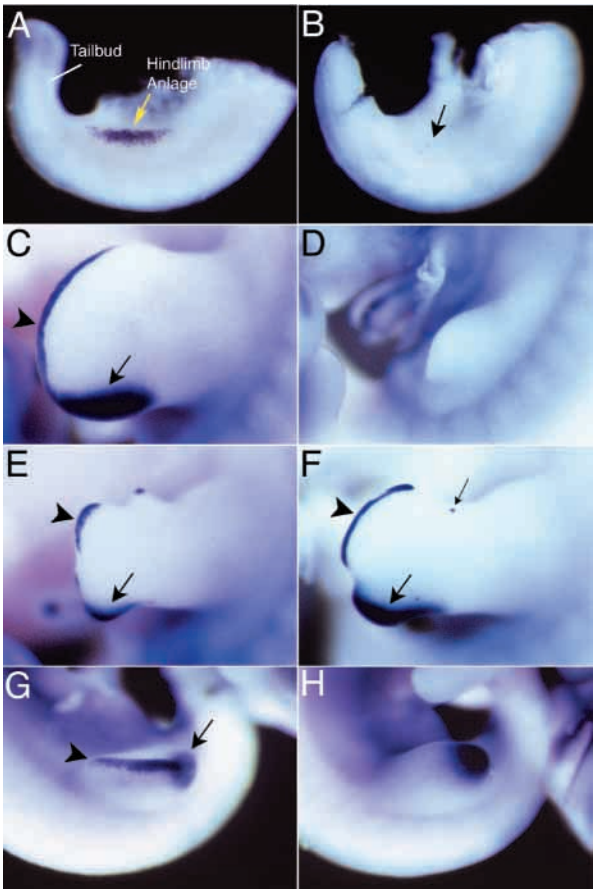

Fig. 5. BMPR-IA is required for apical ectodermal ridge formation. (A-D) *Fgf8* expression was detected in the pre-AER region before overt hindlimb bud development in normal embryos (A; 10.0 dpc), and is a molecular marker for the apical ectodermal ridge at later stages of hindlimb formation (C; 11.5 dpc). *Fgf8* expression was detected in very few cells at 10.0 dpc in most mutant embryos examined (B). Presumably incomplete penetrance of the *Bmpr* conditional knockout allows the expression of *Fgf8* in a small number of cells (arrow). Expression was detected later in hindlimb embryogenesis, but the levels of expression are variable (D-F). (C-F) Hindlimbs (11.5 dpc) double labeled for *Fgf8* expression in the AER (arrowhead) and *Shh* expression in the ZPA (arrow). (C) The normal pattern of *Fgf8* and *Shh* expression. Expression of *Fgf8* and *Shh* varies in the mutant from no expression detected (D; Category '0' in Table 1) to a majority of the pattern detected in normal embryos (F; Category '3' in Table 1). A focal patch of *Fgf8* expression is depicted in F (small arrow). Focal patches were detected that do not lie at the distal tip of the hindlimb, but they were not consistently deflected in either a dorsal or ventral direction. Interestingly, we did not see a ventral extension of AER gene expression, as seen with the *En1* knockouts (Loomis et al., 1998). (G) At 10.5 dpc, *Bmp4* expression is detected in both the ZPA (arrow) and the AER (arrowhead) of normal embryos. (H) *Bmp4* gene expression is variable in the AER of mutant embryos and absent in the embryo depicted. *Bmp4* expression is consistently detected in the ZPA of 10.5 dpc mutants.

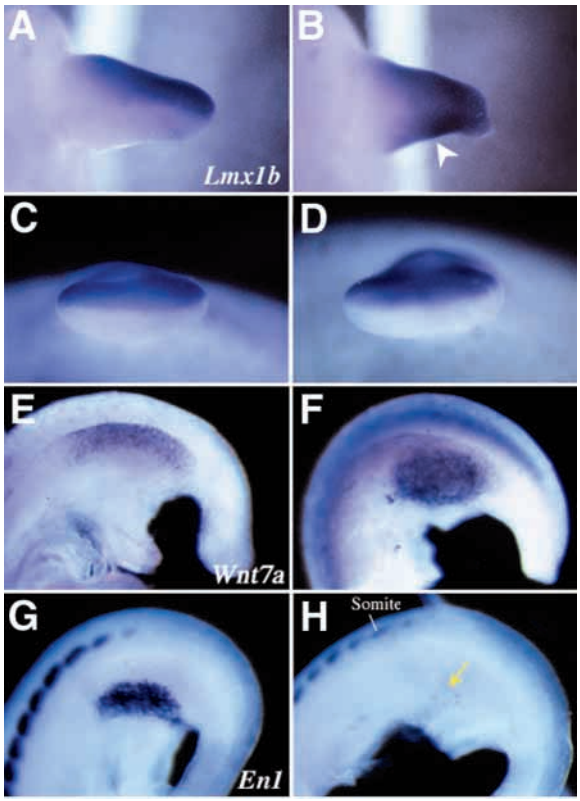

Fig. 6. BMPR-IA is required for dorsal/ventral patterning of the hindlimb. (A,C,E,G) Wild type; (B,D,F,H) mutant. (A-D) *Lmx1b* expression was restricted to dorsal mesoderm in normal 11.5 dpc hindlimb (A). However, the mutant hindlimbs demonstrated a double dorsal phenotype with *Lmx1b* expression being detected in ventral mesoderm (B; arrowhead). *Lmx1b* expression in the mutant forelimb (D) was indistinguishable from the control forelimb (C). (E) *Wnt7a* expression was normally restricted to the dorsal ectoderm of the limb field/bud in a normal 10.25 dpc embryo. (F) *Wnt7a* expression was expanded into the ventral region of the limb field/bud in the *Bmpr* conditional mutants. (G) *En1* expression was restricted to the ventral region of the limb field/bud in a normal 10.25 dpc embryo, which is necessary to suppress *Wnt7a* expression in this region. (H) *En1* expression was almost completely lost in the *Bmpr* conditional mutant. Arrow indicates region where *En1* gene expression should normally exist.

animals that demonstrated agenesis of the limbs (8/35 versus 8/42). Therefore, the variability in hindlimb phenotype correlated with the degree to which the AER formed in the mutants.

Additionally, we observed a similar variability in the expression of other AER markers, including *Bmp4* (Fig. 5G,H) and *Fgf4* (data not shown). In the mutant forelimbs, *Fgf8* expression was largely intact, although the borders of *Fgf8* expression were typically less distinct than the sharp borders detected in normal limbs (data not shown). Rarely, we detected segments of the presumptive AER that failed to express *Fgf8* (data not shown) in the forelimbs. This low incidence of interruptions in *Fgf8* expression may explain the occasional forelimb malformation detected in the mutant animals.

Malformations of the ZPA appear secondary to AER malformations

To examine the status of the anterior/posterior limb organizer, the zone of polarizing activity (ZPA) (Tickle, 1981; Wolpert, 1969), we analyzed the expression of sonic hedgehog (*Shh*) (Krauss et al., 1993; Riddle et al., 1993) in the *Bmpr*

Table 1. Variability of *Fgf8* expression in Bmpr mutant embryos

Age	Data	'0'	'1'	'2'	'3'	'4'	Total
11.5 dpc	*n*	4	7	2	2	0	15
	%	27	47	13	13	0	
10.25-10.5 dpc	*n*	3	6	6	5	0	20
	%	15	30	30	25	0	
Total	*n*	7	13	8	7	0	35
	%	20	37	23	20	0	

The extent of *Fgf8* expression in mutant embryos was characterized by quartiles when compared to normal embryos. '0' corresponded to no expression or only a focal patch of expression whose length was approximately the same size as its width. '4' represents a completely intact *Fgf8* pattern when compared to controls. '1' corresponded to approximately one quarter of the length of the intact *Fgf8* pattern; '2' corresponded to half; and in '3' the *Fgf8* staining pattern corresponded to those embryos in which a clear majority of the *Fgf8* staining pattern was observed. Both the number (*n*) of embryos and the percentage (%) are given.

conditional mutants. We observed a variable expression of *Shh*, which reflected the variability observed with *Fgf8* expression and AER formation (see below). Because *Shh* expression requires the expression of the Fgfs to maintain appropriate expression levels (Laufer et al., 1994; Sun et al., 2000), we hypothesized that the variability of *Shh* expression is dependent on FGF expression in these mutants. To test this directly, we double-labeled embryos with probes against *Fgf8* and *Shh* (Fig. 5C-F). Because the distribution of *Fgf8* expression in the mutants was largely stochastic, the domain of *Shh* expression correlated with the amount of *Fgf8* expression (Fig. 5D-F). However, occasionally a modest domain of *Fgf8* expression would lie directly above the posterior margin of the hindlimb resulting in a robust patch of *Shh* expression (data not shown). These observations are consistent with previous data suggesting that the maintenance of *Shh* expression is dependent on the AER.

Specification of ventral hindlimb is disrupted in *Bmpr* mutants

To assess dorsal/ventral patterning of the limb, we examined the expression of the transcription factor gene, *Lmx1b*. This gene is normally expressed in the dorsal mesenchyme of both the hindlimb bud (Fig. 6A, Fig. 8) and the forelimb bud (Fig. 6C, Fig. 8). In the *Bmpr* conditional mutant, *Lmx1b* was expressed in both the dorsal and ventral mesoderm of the hindlimb, consistent with the double dorsal phenotype observed by histological analyses (Fig. 6B). Expression of *Lmx1b* was restricted to dorsal mesoderm in the mutant forelimb (Fig. 6D) indicating that dorsal/ventral patterning was not disrupted in the forelimb.

Lmx1b expression in the dorsal mesoderm is induced by *Wnt7a* (Cygan et al., 1997; Loomis et al., 1998; Riddle et al., 1995; Vogel et al., 1995), which is expressed in the dorsal ectoderm (Parr and McMahon, 1995) of normal mouse limbs (Fig. 6E, Fig. 8). In *Bmpr* mutant embryos, *Wnt7a* gene expression was expanded ventrally in the hindlimb field (Fig. 6F).

Because previous studies demonstrated that *Wnt7a* expression is repressed in the ventral limb ectoderm by *En1* (Cygan et al., 1997; Loomis et al., 1996; Loomis et al., 1998), we examined *En1* gene expression in the *Bmpr* conditional mutants. As shown in Fig. 6G,H, *En1* expression was virtually lost in mutant embryos. We did not detect substantial *En1* expression at any stage of embryogenesis from 10.0-11.5 dpc, although *En1* expression in the forelimb was normal in the same mutant embryos (data not shown).

Unlike the AER phenotype, the double dorsal phenotype, as assessed by molecular markers, was completely penetrant. All 58 embryos examined with molecular markers of dorsal/ventral patterning demonstrated a double dorsal phenotype in the hindlimb (*En1*, *Lmx1b* and *Wnt7a* probes on embryos 10.25-11.5 dpc). Therefore, these data indicate that BMPR-IA signaling during early limb development is required for the

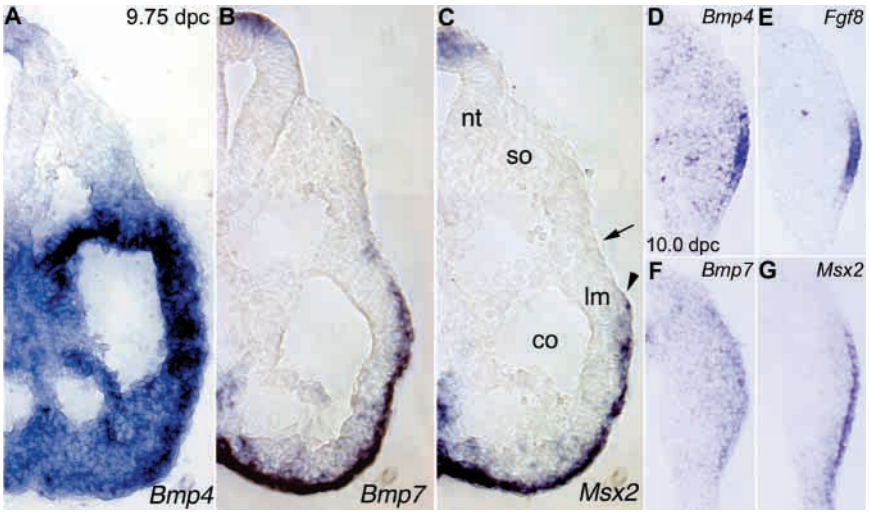

Fig. 7. Expression pattern of gene products that are upstream and downstream of BMPR-IA signaling during early hindlimb development. (A-C) Expression of BMPR-IA ligands, *Bmp4* and *Bmp7*, and their relationship to the domain of *Msx2* expression in normal 9.75 dpc hindlimbs, which is just before limb bud formation. (A) High levels of *Bmp4* expression are detected in tissues of the ventral part of the embryo, including the lateral mesoderm from which the limb mesenchyme develops. (B) *Bmp7* expression is highest in the most ventral region of the embryo in the outermost cell layers. *Bmp7* expression demonstrates a diminishing gradient of expression from ventral to dorsal, and its expression domain ends at the junction of lateral and intermediate mesoderm (indicated by an arrow in C). (C) The *Msx2* expression pattern is similar to that of *Bmp7*, except the dorsal border of expression (arrowhead) does not extend as far dorsomedially (difference between arrow and arrowhead). (D-G) Expression of BMPR-IA ligands, *Bmp4* (D) and *Bmp7* (F), and their relationship to the domain of *Fgf8* (E) and *Msx2* (G) expression in normal 10.0 dpc hindlimb buds. (D,F) The expression of both *Bmp7* and *Bmp4* have been significantly downregulated when compared with their 9.75 dpc expression domain. Furthermore, the *Bmp4* expression domain has been restricted to the pre-AER region as indicated by the expression of pre-AER marker, *Fgf8*, in a serial section (E).

expression of *En1* and therefore, the establishment of ventral limb patterning (Fig. 8).

Expression of *Bmp4* and *Bmp7* correlates with dorsal/ventral patterning and AER formation in the mouse

To assess the role of previously characterized ligands of BMPR-IA during limb development, we examined the expression pattern of *Bmp2*, *Bmp4* and *Bmp7* in the hindlimb at timepoints just before and during the period in which the molecular phenotypes of the *Bmpr* mutants first appeared (Fig. 7). We have observed an extremely dynamic pattern of *Bmp* gene expression during this period. Although *Bmp2* is expressed in the AER at later stages of development (Lyons et al., 1990), we did not detect appreciable levels of expression in the hindlimb during the 9.75-10.0 dpc timeframe (data not shown). At 9.75 dpc, before hindlimb bud formation, *Bmp4* is highly expressed throughout the ventral-lateral part of the embryo, including expression in the lateral mesoderm (Fig. 7A). By 10.0 dpc, the hindlimb bud has begun to form, and *Bmp4* expression has been downregulated in the limb mesoderm (Fig. 7D). Expression levels remain high in the pre-AER region in a pattern that correlates well with the expression of the AER marker, *Fgf8* (Fig. 7D,E). *Bmp7* demonstrates a more restricted pattern of expression than *Bmp4* during the 9.75-10.0 dpc time period. At 9.75 dpc, *Bmp7* expression is detected in the ventral region of the embryo, but is restricted to the outermost region of the embryo within or in close apposition to the ectoderm (Fig. 7B). Interestingly, this expression domain correlates well with the expression domain of *Msx2* at this stage of development (Fig. 7C). By 10.0 dpc, the expression of *Bmp7* has been largely downregulated (Fig. 7F). However, *Msx2* expression retains an expression pattern roughly comparable with that observed at 9.75 dpc (Fig. 7G). These data demonstrate that *Bmp4* and *Bmp7* are expressed in a temporal and spatial sequence that is consistent with the specification of early ventral limb ectoderm, and then rapidly downregulated after limb bud formation is initiated.

DISCUSSION

BMP signaling results in the ventralization of limb ectoderm and formation of the AER

We have demonstrated that BMPR-IA signaling is required during critical steps in the specification of limb ectoderm. Conditional knockout of BMPR-IA function in the ectoderm of the limb prior to limb bud formation disrupts the specification of ventral limb identity and AER formation. It is likely that the DV patterning phenotype is primarily due to the loss of *En1* gene expression, because *En1* has previously been shown to specify ventral pattern in the limb ectoderm. To further assess the role of BMP signaling during early limb development, we examined the expression pattern of the genes encoding the known BMPR-IA ligands, BMP4 and BMP7. These genes demonstrate a dynamic pattern of expression, and are expressed with the correct temporal and spatial sequence to play a role in the specification of ventral limb phenotype and AER induction.

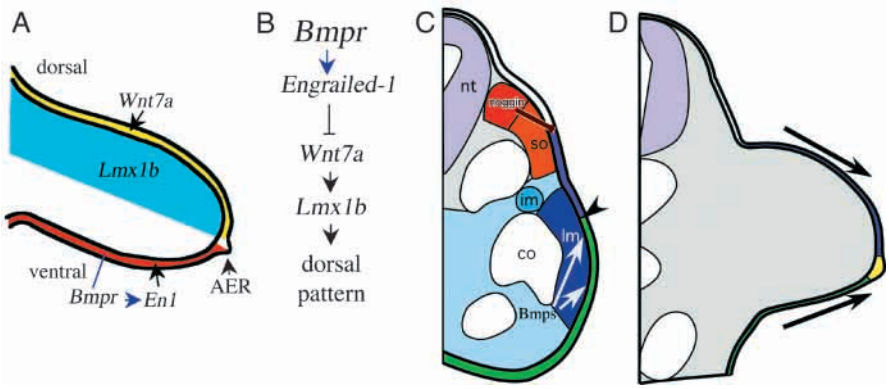

Fig. 8. The hypothesized roles of regulatory genes during limb development. (A) The expression patterns of genes that regulate DV patterning of the limb ectoderm. This schematic depicts a transverse section of the limb bud with proximal to the left, distal to the right ending in the AER, and dorsal towards the top. (B) Model for the genetic pathway regulating dorsal/ventral patterning of the limbs. As shown in this study, *Bmpr* signaling in the limb ectoderm is required for *En1* gene expression (red in A) in the ventral ectoderm. Previous studies have demonstrated a role for *En1* in suppressing the expression of *Wnt7a* (yellow) in ventral ectoderm (Cygan et al., 1997; Loomis et al., 1996; Loomis et al., 1998), thereby restricting its expression to the dorsal ectoderm. *Wnt7a* has been shown to induce the expression of *Lmx1b* (blue) in the mesoderm underlying the dorsal ectoderm (Cygan et al., 1997; Loomis et al., 1998; Riddle et al., 1995). Figure adapted and modified from Johnson and Tabin (Johnson and Tabin, 1997). (C) Hypothesized molecular mechanisms that dictate DV patterning in the presumptive limb region before limb bud formation and the presumptive fate maps of limb ectoderm. Ventral embryonic regions that express *Bmp4* are depicted in various shades of blue with lateral mesoderm (lm) depicted as the darkest shade of blue, and intermediate mesoderm (im) with lighter blue shading. Somitic mesoderm (so) is depicted as red, in those regions that express noggin, and as orange in the remainder of the somite. In the ectoderm, purple denotes regions that correspond to chick ectoderm previously fate mapped to form dorsal limb ectoderm (Altabef et al., 1997; Michaud et al., 1997). Green denotes regions fated to contribute to ventral ectoderm. The arrowhead denotes the boundary between the dorsal and ventral limb compartments (Altabef et al., 1997; Michaud et al., 1997). Our model hypothesizes that the expression of BMPs in the ventral and lateral mesoderm (blue) induce the ventral identity of the overlying ectoderm (green). This induction is blocked by noggin expression in the somite, which previously has been shown to express noggin (Capdevila and Johnson, 1998; Hirsinger et al., 1997; Marcelle et al., 1997; McMahon et al., 1998; Reshef et al., 1998; Tonegawa and Takahashi, 1998). In addition, this region has been demonstrated to induce the overlying ectoderm to form dorsal limb ectoderm (Michaud et al., 1997). Our model proposes that the inhibition of BMP induction in ectoderm overlying the most medial parts of the lateral mesoderm (where purple ectoderm overlies blue mesoderm) is accomplished by noggin. The region of ventral ectoderm hypothesized in this model corresponds to the domain of *Msx2* gene expression, which is lost in the *Bmpr* mutant. (D) Schematic illustration of morphogenetic movements of ectoderm to form dorsal limb ectoderm (purple), AER (yellow) and ventral ectoderm (green).

The mutant phenotype is much more profound in the hindlimb than in the forelimb of the *Bmpr* mutants. Although we cannot rule out the possibility that *En1* expression and DV patterning is differentially regulated in the fore- and hindlimbs, the difference in phenotype between the fore- and hindlimbs most likely results from the difference in the timing and extent of *Bmpr* gene inactivation in the limbs (see Fig. 2A). We hypothesize that DV patterning is established in the forelimb prior to extensive *Bmpr* inactivation, whereas gene inactivation occurs before DV patterning during hindlimb formation. These data would suggest that DV patterning is established in a narrow temporal window just prior to the initial outgrowth of the limb bud. In addition, our observations are consistent with those of Niswander and colleagues, who have shown that BMP signaling is required for DV patterning and AER formation in both the fore- and hindlimbs of chickens (Pizette et al., 2001).

Specification of ventral limb identity

Classical transplantation experiments have demonstrated that mesoderm dictates the DV patterning before limb bud formation, whereas DV patterning is regulated by the ectoderm after the limb bud forms (Chen and Johnson, 1999). In the chicken, the transition of control over DV patterning from the lateral mesoderm to the somatic ectoderm occurs between stages HH14 and HH16 (Geduspan and MacCabe, 1987; Geduspan and MacCabe, 1989). The first indication of limb bud formation occurs with the condensation of lateral mesoderm opposite somites 15-16 at stages HH16 (Hamburger and Hamilton, 1951). The transition from mesodermal to ectodermal control of DV patterning is demonstrated by the fact that a 180º rotation of prospective limb ectoderm at stage HH14 results in a limb with normal DV polarity. However, ectodermal inversion at HH16 results in formation of a limb with reversed DV polarity (Geduspan and MacCabe, 1987; Geduspan and MacCabe, 1989). The acquisition of DV polarity by the ectoderm is accompanied by the expression of genetic regulatory genes, *En1* and *Wnt7a*, at HH15-16 (Davis et al., 1991; Dealy et al., 1993; Gardner and Barald, 1992; Riddle et al., 1995). Mutational analyses in mice have clearly demonstrated that *En1* and *Wnt7a* play complementary roles in specifying ventral and dorsal limb ectoderm, respectively (Fig. 8) (Cygan et al., 1997; Loomis et al., 1996; Loomis et al., 1998; Parr and McMahon, 1995). Therefore, one would predict that candidate factors which regulate the initial induction of DV patterning would be expressed in the lateral mesoderm before limb bud formation and would be required for the induction of factors that specify DV patterning in the overlying ectoderm. Our data demonstrate that ligands of BMPR-IA fulfill these criterion, because *Bmp4* and *Bmp7* are expressed in lateral mesoderm and the overlying ectoderm before limb bud formation, and BMPR-IA signaling is required for the induction of *En1*.

Although classical transplantation analyses have been undertaken in chickens and amphibians, analyses of the cellular and molecular events regulating limb morphogenesis suggest that mechanisms of DV patterning and AER formation are conserved between vertebrates (Johnson and Tabin, 1997; Martin, 1998; Vogt and Duboule, 1999). Specifically, regarding the role of BMP signaling, observations from Niswander and her colleagues (Pizette et al., 2001) are similar, if not identical, to those we have observed in mice. Therefore, our model for BMP signaling will incorporate embryological and molecular observations from all vertebrate model systems.

Although the role of ectoderm in specifying DV patterning after limb bud formation has been well characterized, the precise role of mesoderm before limb bud formation has been less clear, and the molecular mechanisms are completely unknown. In the 1970s, transplantation experiments characterizing the ability of lateral mesoderm to specify early DV patterning were conflicting (Michaud et al., 1997). However, more recent transplantation and cell marking experiments suggest that paraxial mesoderm plays a role in specifying dorsal limb ectoderm, whereas lateral mesoderm specifies ventral limb ectoderm (Altabef et al., 1997; Michaud et al., 1997). The conclusions from these studies is incorporated into the model schematized in Fig. 8C,D. For example, Michaud et al. demonstrated that an 180º inversion of lateral mesoderm alone at pre-limb bud stages (HH12-13) (dark blue in Fig. 8C) does not result in an inversion of limb polarity (Michaud et al., 1997). However, inversions of both lateral and somitic mesoderm (dark blue and red/orange, respectively, in Fig. 8C) does invert DV polarity of the resulting limbs. In addition, transplantation of an ectopic somite into lateral mesoderm, such that the lateral mesoderm was flanked by the endogenous somite medially and the ectopic somite laterally, resulted in the formation of a bidorsal limb. These data and other data suggested that a dorsalizing signal was emanating from the somitic mesoderm, and a ventralizing signal emanated from the lateral mesoderm.

If the dorsalizing signal emanates from the somitic mesoderm, how then does this give rise to dorsal limb ectoderm? Both transplantation (Michaud et al., 1997) and cell labeling experiments (Altabef et al., 1997), demonstrate that ectoderm overlying the somites are fated to become dorsal limb ectoderm (depicted as purple ectoderm in Fig. 8C,D). Tickle and colleagues have undertaken cell fate mapping experiments that demonstrate a large fraction of dorsal limb ectoderm originates from the ectoderm overlying the somites (Altabef et al., 1997). These data suggest that the ectoderm overlying the somites is fated to become dorsal limb ectoderm, and then morphogenetic movements result in the translocation of this ectoderm such that it covers the dorsal limb (as schematized in Fig. 8D).

A molecular model for epithelial-mesenchymal interactions during early limb development

Our model hypothesizes that BMP signaling pathway mediates the initial induction of DV pattern in the presumptive limb ectoderm before limb bud formation. *Bmp4* and *Bmp7* are expressed in the lateral mesoderm and the overlying ectoderm just prior to the induction of limb bud formation, and therefore are correctly positioned in both time and space to induce ventral limb ectoderm (Fig. 7, Fig. 8). Furthermore, we have demonstrated that BMPR-IA signaling is required for the induction of *En1*, and subsequently the specification of ventral limb identity. Finally, the dorsalizing effect of somites, we hypothesize, is mediated by the expression of the BMP antagonist, noggin, in the myotomal compartment of the somite (Capdevila and Johnson, 1998; Hirsinger et al., 1997; Marcelle et al., 1997; McMahon et al., 1998; Reshef et al., 1998; Tonegawa and Takahashi, 1998). Noggin expression in

the somites could explain the ability of somites to dorsalize the ectoderm in transplantation experiments because of their ability to inhibit BMP signals from the lateral mesoderm. Noggin expressed in the somites could neutralize the effects of BMPs in the ectoderm that is in close apposition to the somites (Fig. 8C). Alternatively, the somitic mesoderm could induce the expression of an unidentified BMP antagonist in dorsal ectoderm, which suppresses the BMP signaling within the dorsal ectoderm itself.

Finally, the mesoderm-derived inductive signal would have to be downregulated as the lateral mesoderm loses its ability to induce the overlying ectoderm and as the dorsally fated ectoderm moves over the limb mesenchyme. Our analyses demonstrate that the expression of *Bmp4* and *Bmp7* are rapidly downregulated in most of the lateral mesenchyme as the limb bud is formed (Fig. 7D,F), although *Bmp4* expression is maintained in the distal limb where BMP signaling is required for AER formation.

Role of BMPR-IA signaling during AER formation

Our data demonstrate a crucial role for BMPR-IA signaling in the formation of the AER. It is conceivable that the AER defects are secondary to DV patterning defects. However, this seems unlikely because the penetrance of the DV patterning defect is complete, whereas the AER defect is quite variable. This difference in penetrance argues that AER formation and DV patterning are two independent processes. Our argument is further bolstered by analyses of the *eudiplopodia* chick mutant that suggest that AER formation is not strictly dependent on establishment of a DV border at the distal tip of the limb (Laufer et al., 1997).

Classical studies have shown that lateral mesoderm induces the AER (Carrington and Fallon, 1984; Saunders and Reuss, 1974). As *Bmp4* and *Bmp7* are expressed in lateral mesoderm, they are candidates for the initial inductive event required for AER formation.

There are mutants, such as *limbless*, in which both AER formation and DV patterning are affected. One parsimonious explanation is that the *limbless* gene product may be epistatic to BMP signaling and therefore affects both independent processes because they are mediated by one signaling pathway. An additional mutant that affects both DV patterning and AER formation is the *En1* knockout. In this case, there are important differences between the *Bmpr* mutant and the *En1* mutant. Most importantly, the *En1* knockout does not abrogate AER formation, but does affect the positioning of the AER. *En1* mutants demonstrate a ventral extension of the AER (Loomis et al., 1996; Loomis et al., 1998). The AER, where it is formed in the *Bmpr* mutant, does not demonstrate the ventral extension seen in *En1* mutants (Fig. 5; data not shown). Michaud et al. also did not observe a ventral extension of the AER in double dorsal phenotypes generated by transplantation experiments in chick (Michaud et al., 1997). These data, in conjunction with our data, suggest that the ventral AER extension is not a consistent feature of the double dorsal phenotype.

In summary, the conditional knockout of the gene for the most widely expressed type I BMP receptor, BMPR-IA, results in limb malformations that are due to the disruption of AER formation and loss of DV patterning. This is the first demonstration that BMPR-IA signaling is essential for these early events in limb morphogenesis.

We thank C. W. Ragsdale and T. A. Sanders for providing us their whole-mount in situ hybridization protocol prior to publication; L. Niswander for providing results prior to publication; S. O'Gorman for the Cre expression plasmid; A. Joyner, A. McMahon, D. Phippard, R. Johnson, R. Riddle for probes; and J. Golden for help with vibratome sectioning. We would also like to thank R. Riddle for advice on the limb analyses and for reading the manuscript; Randy Johnson for comments on the manuscript. E. B. C.'s and R. R. B.'s laboratories are supported by the NIH.

REFERENCES

Altabef, M., Clarke, J. D. and Tickle, C. (1997). Dorso-ventral ectodermal compartments and origin of apical ectodermal ridge in developing chick limb. *Development* **124**, 4547-4556.

Arango, N. A., Lovell-Badge, R. and Behringer, R. R. (1999). Targeted mutagenesis of the endogenous mouse Mis gene promoter: in vivo definition of genetic pathways of vertebrate sexual development. *Cell* **99**, 409-419.

Capdevila, J. and Johnson, R. L. (1998). Endogenous and ectopic expression of noggin suggests a conserved mechanism for regulation of BMP function during limb and somite patterning. *Dev. Biol.* **197**, 205-217.

Carrington, J. L. and Fallon, J. F. (1984). The stages of flank ectoderm capable of responding to ridge induction in the chick embryo. *J. Embryol. Exp. Morphol.* **84**, 19-34.

Chen, H. and Johnson, R. L. (1999). Dorsoventral patterning of the vertebrate limb: a process governed by multiple events. *Cell Tissue Res.* **296**, 67-73.

Chen, H., Lun, Y., Ovchinnikov, D., Kokubo, H., Oberg, K. C., Pepicelli, C. V., Gan, L., Lee, B. and Johnson, R. L. (1998). Limb and kidney defects in Lmx1b mutant mice suggest an involvement of LMX1B in human nail patella syndrome. *Nat. Genet.* **19**, 51-55.

Cho, H., Mu, J., Kim, J. K., Thorvaldsen, J. L., Chu, Q., Crenshaw, E. B., 3rd, Kaestner, K. H., Bartolomei, M. S., Shulman, G. I. and Birnbaum, M. J. (2001). Insulin resistance and a diabetes mellitus-like syndrome in mice lacking the protein kinase Akt2 (PKB beta). *Science* **292**, 1728-1731.

Cohn, M. J., Izpisua-Belmonte, J. C., Abud, H., Heath, J. K. and Tickle, C. (1995). Fibroblast growth factors induce additional limb development from the flank of chick embryos. *Cell* **80**, 739-746.

Crossley, P. H., Minowada, G., MacArthur, C. A. and Martin, G. R. (1996). Roles for FGF8 in the induction, initiation, and maintenance of chick limb development. *Cell* **84**, 127-136.

Cygan, J. A., Johnson, R. L. and McMahon, A. P. (1997). Novel regulatory interactions revealed by studies of murine limb pattern in Wnt-7a and En-1 mutants. *Development* **124**, 5021-5032.

Davis, C. A., Holmyard, D. P., Millen, K. J. and Joyner, A. L. (1991). Examining pattern formation in mouse, chicken and frog embryos with an En-specific antiserum. *Development* **111**, 287-298.

Dealy, C. N., Roth, A., Ferrari, D., Brown, A. M. and Kosher, R. A. (1993). Wnt-5a and Wnt-7a are expressed in the developing chick limb bud in a manner suggesting roles in pattern formation along the proximodistal and dorsoventral axes. *Mech. Dev.* **43**, 175-186.

Dreyer, S. D., Zhou, G., Baldini, A., Winterpacht, A., Zabel, B., Cole, W., Johnson, R. L. and Lee, B. (1998). Mutations in LMX1B cause abnormal skeletal patterning and renal dysplasia in nail patella syndrome. *Nat. Genet.* **19**, 47-50.

Echelard, Y., Epstein, D. J., St-Jacques, B., Shen, L., Mohler, J., McMahon, J. A. and McMahon, A. P. (1993). Sonic hedgehog, a member of a family of putative signaling molecules, is implicated in the regulation of CNS polarity. *Cell* **75**, 1417-1430.

Gardner, C. A. and Barald, K. F. (1992). Expression patterns of engrailed-like proteins in the chick embryo. *Dev. Dyn.* **193**, 370-388.

Geduspan, J. S. and MacCabe, J. A. (1987). The ectodermal control of mesodermal patterns of differentiation in the developing chick wing. *Dev. Biol.* **124**, 398-408.

Geduspan, J. S. and MacCabe, J. A. (1989). Transfer of dorsoventral information from mesoderm to ectoderm at the onset of limb development. *Anat. Rec.* **224**, 79-87.

Hamburger, V. and Hamilton, H. L. (1951). A series of normal stages in the development of chick embryos. *J. Morphol.* **88**, 49-92.

Heydemann, A., Nguyen, L. C. and Crenshaw III, E. B. (2001). A regulatory region of the *Brn4/Pou3f4* promoter directs expression to developing forebrain and neural tube. *Dev. Brain Res.* **128**, 83-90.

Hirsinger, E., Duprez, D., Jouve, C., Malapert, P., Cooke, J. and Pourquie,

O. (1997). Noggin acts downstream of Wnt and Sonic Hedgehog to antagonize BMP4 in avian somite patterning. *Development* **124**, 4605-4614.
Hogan, B., Beddington, R., Costantini, F. and Lacy, E. (1994). Manipulating the mouse embryo: a laboratory manual. Plainview, NY: Cold Spring Harbor Laboratory Press.
Hogan, B. L. (1996). Bone morphogenetic proteins: multifunctional regulators of vertebrate development. *Genes Dev.* **10**, 1580-1594.
Johnson, R. L. and Tabin, C. J. (1997). Molecular models for vertebrate limb development. *Cell* **90**, 979-990.
Krauss, S., Concordet, J. P. and Ingham, P. W. (1993). A functionally conserved homolog of the Drosophila segment polarity gene hh is expressed in tissues with polarizing activity in zebrafish embryos. *Cell* **75**, 1431-1444.
Laufer, E., Nelson, C. E., Johnson, R. L., Morgan, B. A. and Tabin, C. (1994). Sonic hedgehog and Fgf-4 act through a signaling cascade and feedback loop to integrate growth and patterning of the developing limb bud. *Cell* **79**, 993-1003.
Laufer, E., Dahn, R., Orozco, O. E., Yeo, C. Y., Pisenti, J., Henrique, D., Abbott, U. K., Fallon, J. F. and Tabin, C. (1997). Expression of Radical fringe in limb-bud ectoderm regulates apical ectodermal ridge formation. *Nature* **386**, 366-373.
Logan, C., Hanks, M. C., Noble-Topham, S., Nallainathan, D., Provart, N. J. and Joyner, A. L. (1992). Cloning and sequence comparison of the mouse, human, and chicken engrailed genes reveal potential functional domains and regulatory regions. *Dev. Genet.* **13**, 345-358.
Loomis, C. A., Harris, E., Michaud, J., Wurst, W., Hanks, M. and Joyner, A. L. (1996). The mouse Engrailed-1 gene and ventral limb patterning. *Nature* **382**, 360-363.
Loomis, C. A., Kimmel, R. A., Tong, C. X., Michaud, J. and Joyner, A. L. (1998). Analysis of the genetic pathway leading to formation of ectopic apical ectodermal ridges in mouse Engrailed-1 mutant limbs. *Development* **125**, 1137-1148.
Lyons, K. M., Pelton, R. W. and Hogan, B. L. (1990). Organogenesis and pattern formation in the mouse: RNA distribution patterns suggest a role for bone morphogenetic protein-2A (BMP-2A). *Development* **109**, 833-844.
Mahmood, R., Bresnick, J., Hornbruch, A., Mahony, C., Morton, N., Colquhoun, K., Martin, P., Lumsden, A., Dickson, C. and Mason, I. (1995). A role for FGF-8 in the initiation and maintenance of vertebrate limb bud outgrowth. *Curr. Biol.* **5**, 797-806.
Marcelle, C., Stark, M. R. and Bronner-Fraser, M. (1997). Coordinate actions of BMPs, Wnts, Shh and noggin mediate patterning of the dorsal somite. *Development* **124**, 3955-3963.
Martin, G. R. (1998). The roles of FGFs in the early development of vertebrate limbs. *Genes Dev.* **12**, 1571-1586.
Massague, J. (1998). TGF-beta signal transduction. *Annu. Rev. Biochem.* **67**, 753-791.
McMahon, J. A., Takada, S., Zimmerman, L. B., Fan, C. M., Harland, R. M. and McMahon, A. P. (1998). Noggin-mediated antagonism of BMP signaling is required for growth and patterning of the neural tube and somite. *Genes Dev* **12**, 1438-1452.
Michaud, J. L., Lapointe, F. and Le Douarin, N. M. (1997). The dorsoventral polarity of the presumptive limb is determined by signals produced by the somites and by the lateral somatopleure. *Development* **124**, 1453-1463.
Mishina, Y., Suzuki, A., Ueno, N. and Behringer, R. R. (1995). Bmpr encodes a type I bone morphogenetic protein receptor that is essential for gastrulation during mouse embryogenesis. *Genes Dev.* **9**, 3027-3037.
Nagy, A. (2000). Cre recombinase: the universal reagent for genome tailoring. *Genesis* **26**, 99-109.
Niswander, L. and Martin, G. R. (1993). FGF-4 and BMP-2 have opposite effects on limb growth. *Nature* **361**, 68-71.
Niswander, L., Tickle, C., Vogel, A., Booth, I. and Martin, G. R. (1993). FGF-4 replaces the apical ectodermal ridge and directs outgrowth and patterning of the limb. *Cell* **75**, 579-587.
Parr, B. A. and McMahon, A. P. (1995). Dorsalizing signal Wnt-7a required for normal polarity of D-V and A-P axes of mouse limb. *Nature* **374**, 350-353.
Parr, B. A., Shea, M. J., Vassileva, G. and McMahon, A. P. (1993). Mouse Wnt genes exhibit discrete domains of expression in the early embryonic CNS and limb buds. *Development* **119**, 247-261.
Phippard, D., Lu, L., Lee, D., Saunders, J. C. and Crenshaw III, E. B. (1999). Targeted mutagenesis of the POU-domain gene, *Brn4/Pou3f4*, causes development defects in the inner ear. *J. Neurosci.* **19**, 5980-5989.
Phippard, D. J., Heydemann, A., Lechner, M., Lu, L., Lee, D., Kyin, T. and Crenshaw III, E. B. (1998). Changes in the subcellular localization of the *Brn4* gene product precede mesenchymal remodeling of the otic capsule. *Hear. Res.* **120**, 77-85.
Pizette, S., Abate-Shen, C. and Niswander, L. (2001). BMP controls proximodistal outgrowth, via induction of the apical ectodermal ridge, and dorsoventral patterning of the vertebrate limb. *Development* **128**, 4463-4474.
Reshef, R., Maroto, M. and Lassar, A. B. (1998). Regulation of dorsal somitic cell fates: BMPs and Noggin control the timing and pattern of myogenic regulator expression. *Genes Dev.* **12**, 290-303.
Riddle, R. D., Ensini, M., Nelson, C., Tsuchida, T., Jessell, T. M. and Tabin, C. (1995). Induction of the LIM homeobox gene Lmx1 by WNT7a establishes dorsoventral pattern in the vertebrate limb. *Cell* **83**, 631-640.
Riddle, R. D., Johnson, R. L., Laufer, E. and Tabin, C. (1993). Sonic hedgehog mediates the polarizing activity of the ZPA. *Cell* **75**, 1401-1416.
Saunders, J. W., Jr (1948). The proximo-distal sequences of origin of the parts of the chick wing and the role of ectoderm. *J. Exp. Zool.* **108**, 363-404.
Saunders, J. W. J. and Reuss, C. (1974). Inductive and axial properties of prospective wing-bud mesoderm in the chick embryo. *Dev. Biol.* **38**, 41-50.
Soriano, P. (1999). Generalized lacZ expression with the ROSA26 Cre reporter strain. *Nat. Genet.* **21**, 70-71.
Sun, X., Lewandoski, M., Meyers, E. N., Liu, Y.-H., Maxson, R. E. and Martin, G. R. (2000). Conditional inactivation of Fgf4 reveals complexity of signalling during limb bud development. *Nat. Genet.* **25**, 83-86.
Tickle, C. (1981). The number of polarizing region cells required to specify additional digits in the developing chick wing. *Nature* **289**, 295-298.
Tickle, C. and Altabef, M. (1999). Epithelial cell movements and interactions in limb, neural crest and vasculature. *Curr. Opin. Genet. Dev.* **9**, 455-460.
Tonegawa, A. and Takahashi, Y. (1998). Somitogenesis controlled by Noggin. *Dev. Biol.* **202**, 172-182.
Vogel, A., Rodriguez, C., Warnken, W. and Izpisua Belmonte, J. C. (1995). Dorsal cell fate specified by chick Lmx1 during vertebrate limb development. *Nature* **378**, 716-720.
Vogel, A., Rodriguez, C. and Izpisua-Belmonte, J. C. (1996). Involvement of FGF-8 in initiation, outgrowth and patterning of the vertebrate limb. *Development* **122**, 1737-1750.
Vogt, T. F. and Duboule, D. (1999). Antagonists go out on a limb. *Cell* **99**, 563-566.
Wilkinson, D. G. (1992). In situ hybridization: a practical approach. In *A Practical Approach Series* (ed. D. Rickwood and B. D. Hames), pp. 75-83. New York: Oxford University Press.
Wolpert, L. (1969). Positional information and the spatial pattern of cellular differentiation. *J. Theor. Biol.* **25**, 1-47.